SEMARAK ILMU PUBLISHING

Journal of Advanced Research in Fluid Mechanics and Thermal Sciences

Journal homepage:
https://semarakilmu.com.my/journals/index.php/fluid_mechanics_thermal_sciences/index
ISSN: 2289-7879

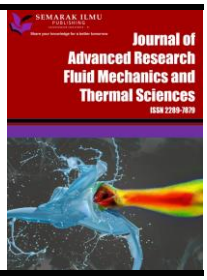

Numerical Study of Hydrothermal Enhancement of Two-Phase Flow in a Vertical Pipe by using Modified Vortex Generators

Fawzi Shnain Alnasur[1,*], Riyadh Sabah Alturaihi[2]

[1] Environmental Research and Pollution Prevention Unit, College of Science, Al-Qadisiyah University, Al-Qadisiyah, Iraq
[2] Department of Mechanics, College of Engineering, University of Babylon, Babylon, Iraq

ARTICLE INFO

Article history:
Received 20 July 2024
Received in revised form 28 October 2024
Accepted 10 November 2024
Available online 30 November 2024

Keywords:
Twisted tape; two-phase flow; wavy edge; thermal enhancement; swirl flow

ABSTRACT

The improvement in heat transfer and energy savings in two-phase (gas-liquid) flow in tubes occupies a wide area of research interest. In this work, the effect of modified twisted tape turbulators on heat transfer augmentation in vertical tubes is studied numerically by using the CFD technique. A vortex generator (twisted tape) was used as a passive method to raise the rate of heat transfer. The variants of the water flow rate, air flow rate, heat flux, and twisted ratio of a twisted tape tabulator were considered. This work provides a superficial water Re No. With ranges of 6300–10500, considering three different water and airflow rates. Additionally, the superficial gas Re range was 6000-16000. Three distinct twist ratios (TR) of 7.8, 3.9, and 2.6 were considered for the iron twisted tape to examine the impact of the twist ratio on the tube's thermo-hydraulic characteristics. The test section consisted of an insulated copper vertical tube subjected to three constant heat fluxes. This paper investigated three variants: the friction factor, Nusselt number, and performance evaluation factor. A strong turbulent vortex flow with an increase in secondary flow in the tube's radial direction was significantly intensified in the presence of the twisted tape inserted. Also, an increase in Reynold's number for both water and air and increased heat flux led to a proportional increase in heat transfer while the friction factor decreased. The presence of the modified twisted tape showed an improvement in the heat transfer and the pressure loss reduction when compared with the plain tape for all twisting ratios and for all cases where the highest value of the performance evaluation factor was two at the twisted ratio of 2.6 with an increase percentage of 81%. Conclusively, this investigation concludes that using modified twisted tape can greatly enhance the heat transfer rates and reduce pressure resistance, increasing the performance evaluation factor of heat exchanger systems.

1. Introduction

Researchers are looking into ways to improve the efficiency of energy systems due to consumerism and the limitations placed on energy sources [1,2]. Heat exchanger-based energy systems have drawn much attention because they are essential to using and transferring energy [3,4]. For engineers and researchers working on thermal systems, improving the performance of heat

* *Corresponding author.*
E-mail address: fawzi.shnain@qu.edu.iq

https://doi.org/10.37934/arfmts.124.2.1338

exchangers has grown in importance and interest [5]. Active and passive heat transfer enhancement techniques are the two main categories, and their classification is based on real-world applications. [6]. Active techniques to improve the heat transfer coefficient depend on external force, representing additional energy consumption, which is the main negative point of this technique [7].

On the other hand, passive methods are those where the main means of improving the heat transfer is through surface modification, coiled tubes (augmented, rough, and extended) surfaces, liquid additives, and swirl flow devices, such as twisted ducts, twisted tape and ribs, and other modifications without any energy consumption, so it is better to use and improve them [8]. The twisted tapes as a passive method have attracted research attention in recent years due to their high thermal performance and compact structure, ease and low cost of manufacture in different sizes, shapes, and suitability for the types of flow [9].

These extensive studies of heat transfer via two-phase flow are connected to the research by Bhagwat and Ghajar [10] and Khorasani and Dadvand [11]. Their research discovered that the form, shape, orientation, flow pattern, and other factors of the tube are all strictly related to the thermo-hydraulic properties of the air/water two-phase flow. Additionally, they noted that the two-phase flow's heat transfer coefficient increases noticeably with an increase in the gas Reynolds number. The use of twisted tapes has drawn much interest in passive techniques [12]. The Reynolds number and heat transfer coefficient are raised by the twisted tape turbulators, which create swirling flows inside the mainstream [13]. Different kinds of plain twisted tapes, double-twisted tapes, and cut-twisted tapes have all been proposed by researchers [14-16].

In order to increase heat transmission, three alternative strategies were employed: wave-strip turbulator (WST), gas bubble injection, and water-CuO nanofluid [17]. When applying the three adjustments simultaneously, the thermal transmission increased from 33% to 144%. The results demonstrated that the vortex generators raised heat transfer to 17%. The pressure drop for the two-phase boiling flow of the refrigerant R-407C was experimentally investigated by Jadhav *et al.,* [18]. Employing the plain twisted tape inserted in the horizontal pipe with (TR = 9, 14) and varying heat flux range and refrigerant mass flux. The findings demonstrated that at TR = 9, the pressure losses reached their highest value due to increased turbulence. The experimental investigation on two-phase (air-water) flow in a pipe with discrete ribs positioned on an angle to the twisted tape axis covered by Tarasevich *et al.,* [19] led to increased heat transfer from 14% to 21%. By utilizing the plain twisted tape turbulators and air bubble injection, Pourahmad *et al.,* [20] integrate passive and active approaches to improve the flow's thermal efficiency in pipes. Comparing the Nu number to all other cases, using both approaches together can boost it by (98 to 114%, 3 to 14%, and 20 to 39%). The effects of using twisted tapes with twisted ratio =4, 10, and 15 in a horizontal tube with the two-phase flow (x = 0.1–0.7) for isobutane (R600a) condensation were covered by Moghaddam *et al.,* [21]. The tube set TTI (twisted ratio =10) yielded the best performance, increasing the performance factor from 0.39 to 1.05. In their experimental study of the condensation flow through plain and twisted cassette tubes, Sajadi *et al.,* [22] used the R1234yf as the working medium with TR = 6, 9, and 12. Based on the fulfilment of (TR = 6), the highest increment in h was found to be 42%, and the maximum increment in the pressure drop was 235%. In their experimental discussion of using plain twisted tape to promote the transfer of heat for a heat exchanger using two-phase flow, Sarmadian *et al.,* [23] employed a horizontal copper channel test evaporator with TR (4, 10, and 15) applied at (x = 0.1 to 0.8). The working fluid was R600a. The experiment's findings demonstrated that the performance factor varied from 0.44 to 1.09 when twisted tape was used. Yan *et al.,* [24] studied the CHF of boiling subcooled water via a tube with a vertical position. The twisted tape was inserted and heated. The findings demonstrate that when TRs 2 and 4 were applied, CHFs in twisted-tape tubes improved to 1.25 and 1.75 times, respectively, better than those in smooth tubes.

The primary goal of this study was to enhance convective heat transfer by altering the geometry of the twisted ribbons and choosing the optimal design to minimize the pressure drop and maximize the heat transfer in two-phase flow across tubes fitted with twisted tape by increasing turbulence intensity and higher mixing of liquid. Considering the literature review above, thus far, there has been no research available, both theoretically and experimentally, that can consider the twisted tape's wavy edge when inserting the vertical pipe with a two-phase flow. Consequently, this work attempts to close this gap and explore the effect of the modified twisted stripe inside tubes on heat transfer. The present work has been done with three different geometrical cases, namely: (i) a pipe without a twisted stripe, (ii) a pipe with a plain twisted stripe, and (iii) a pipe with a modified twisted stripe with a wavy edge. The effects of water and airflow velocities, twisted ratio, and heat flux on the Nusselt number, friction factor, and performance evaluation factor have been analyzed for all cases. Thus, it would be important to comprehend the impact of the abovementioned modifications on the two-phase flow applications in many thermal industrial processes, such as heat exchangers.

2. Mathematical Analysis

2.1 Governing Equations

The formula for governing equations for mass (continuity), momentum (in 3D), and energy equations were as follows [25]

Continuity equation

$$\frac{\partial \mathrm{u}}{\partial \mathrm{x}}+\frac{\partial \mathrm{v}}{\partial \mathrm{y}}+\frac{\partial \mathrm{w}}{\partial \mathrm{z}}=0 \tag{1}$$

Momentum equations in 3-D (x, y, z)

In X-D: $$u\frac{\partial u}{\partial x}+v\frac{\partial u}{\partial y}+w\frac{\partial u}{\partial z}=-\frac{1}{\rho}\frac{\partial p}{\partial x}+\frac{\mu}{\rho}\left(\frac{\partial^2 u}{\partial x^2}+\frac{\partial^2 u}{\partial y^2}+\frac{\partial^2 u}{\partial z^2}\right) \tag{2}$$

In Y-D: $$u\frac{\partial v}{\partial x}+v\frac{\partial v}{\partial y}+w\frac{\partial v}{\partial z}=-\frac{1}{\rho}\frac{\partial p}{\partial y}+\frac{\mu}{\rho}\left(\frac{\partial^2 v}{\partial x^2}+\frac{\partial^2 v}{\partial y^2}+\frac{\partial^2 v}{\partial z^2}\right) \tag{3}$$

In Z-D: $$u\frac{\partial w}{\partial x}+v\frac{\partial w}{\partial y}+w\frac{\partial w}{\partial z}=-\frac{1}{\rho}\frac{\partial p}{\partial z}+\frac{\mu}{\rho}\left(\frac{\partial^2 w}{\partial x^2}+\frac{\partial^2 w}{\partial y^2}+\frac{\partial^2 w}{\partial z^2}\right) \tag{4}$$

Energy equation

$$\mathrm{u}\frac{\partial \mathrm{T_f}}{\partial \mathrm{x}}+\mathrm{v}\frac{\partial \mathrm{T_f}}{\partial \mathrm{y}}+\mathrm{w}\frac{\partial \mathrm{T_f}}{\partial \mathrm{z}}=\frac{\mathrm{k}}{\rho \mathrm{cp}}\left(\frac{\partial^2 \mathrm{T_f}}{\partial \mathrm{x}^2}+\frac{\partial^2 \mathrm{T_f}}{\partial \mathrm{y}^2}+\frac{\partial^2 \mathrm{T_f}}{\partial \mathrm{z}^2}\right) \tag{5}$$

2.2 Turbulent Model

The turbulent flow model was the Realizable k-ε with Thermal near-the Wall Treatment (R k-ε EWT), which was used for swirling flow because [11]

There are two key distinctions between the standard model and the realizable model:

i. A different turbulent viscosity formula is included in the realizable model.
ii. An exact formula for the transport of the mean-square vorticity fluctuation was used to create the modified transport equation for the dissipation rate.

The term "realizable" refers to the model's ability to satisfy specific mathematical restrictions on the Reynolds stresses, which is in line with the workings of swirling turbulent flows, which distinguishes this model. Represented in the Eq. (6) and Eq. (7) [26].

$$\frac{\partial}{\partial x_j}(\rho k u_j = \frac{\partial}{\partial x_j}[\left(\mu + \frac{\mu_t}{\sigma_k}\right)\frac{\partial k}{\partial x_j}] + G_k + G_b - \rho\varepsilon - Y_M + S_k \quad (6)$$

$$\frac{\partial}{\partial x_j}(\rho \varepsilon u_j = \frac{\partial}{\partial x_j}[\left(\mu + \frac{\mu_t}{\sigma_\varepsilon}\right)\frac{\partial \varepsilon}{\partial x_j}] + \rho C_1 S_\varepsilon - \rho C_2 \frac{\varepsilon^2}{k+\sqrt{\vartheta\varepsilon}} + C_1\varepsilon\frac{\varepsilon}{k}C_3 G_b + S_\varepsilon \quad (7)$$

where

$$C_1 = Max\left[0.43\frac{\eta}{\eta+5}\right],\ \eta = S\frac{K}{\varepsilon}\ ,\ S = \sqrt{2S_{ij}}$$

G_k generated turbulence kinetic energy due to the mean velocity gradients. G_b was a generation of turbulence kinetic energy due to buoyancy. Y_m represents the contribution of the fluctuating dilatation in compressible turbulence to the overall dissipation rate. C_2, C_1, and ε were constants. σ_k and σ_ε were the turbulent Prandtl numbers for k and ε, respectively. S_k and S_ε were user-defined source terms. The model constants were:

$$C_{1\varepsilon} = 1.4, C_1 = 1.9, \sigma_k = 1, \sigma_3 = 1.2$$

2.3 Data Reduction

To calculate the hydrothermal parameters for fluids flow in a tube, we can use the following expressions Eq. (8) to Eq. (14) [27]:

$$f = \frac{\Delta P}{(L/D)((\rho_m v^2)/2)} \quad (8)$$

where f is the friction factor, ΔP is the pressure difference between the inlet and outlet of a test tube.

$$\Delta p = p_{in} - p_{out} \quad (9)$$

P_{in} and P_{out} were the tube inlet and outlet pressures.

A dimensionless parameter, Reynolds number, is used to measure the velocity of fluids, mass flow rate, and the fluids flow types, which can be calculated using Eq. (10) [27].

$$\mathrm{Re} = \frac{\rho_m * u * D_h}{\mu_m} \quad (10)$$

A dimensionless parameter average Eq. (11) can be used to calculate the Nusselt number, a crucial parameter for assessing convective heat transfer performance [25].

$$Nu = \frac{h * D_h}{k_m} \quad (11)$$

k_m was the fluid's thermal conductivity, D_h was the hydraulic diameter, and h was the convective heat transfer coefficient, which can be calculated using Eq. (12) [25].

$$h_{\text{ave}} = \frac{q_f}{A_{\text{con.}}\,(T_w - T_b)} \tag{12}$$

where, $A_{con.}$, the area of convection heat transfer (test tube wall), T_w average temperature of the test tube wall, and T_b average fluid temperature of the mixture. q_f The amount of heat the fluid gains from the pipe's hot walls can be calculated using Eq. (13) [25].

$$q_f = m^{\circ} Cp_m (T_o - T_{in}) \tag{13}$$

where T_o T_{in} were a fluid temperature at outlet and inlet, respectively.

The overall hydrothermal heat enhancement can be evaluated using a suitable index named the Performance Evaluation Factor (PEF), which is related to the heat convective and pressure loss along the stream, so this factor can be defined as Eq. (14) [25]:

$$PEF = (\frac{Nu}{Nu_{\circ}})/(\frac{f}{f_{\circ}})^{1/3} \tag{14}$$

where $Nu_{\circ}$,$f_{\circ}$ The test tube's Nusselt number and friction factor were not twisted.

3. Numerical Simulations

3.1 Physical Modeling

A 3D numerical modelling and conjugate heat transfer simulation was solved with the finite-element method based on the CFD software package ANSYS Fluent 2022 R1, which solves coupled hydrothermal problems like multiphase phenomena. The numerical model consists of an entrance tube connected to a copper test tube that was assumed to be completely thermally insulated, in which two types of twisted tapes were inserted into the test tube (normal and modified made from iron with three twisting ratios TR1=7.8, TR2= 3.9 and TR3=2.6) respectively for each type. Figure 1 shows the entrance, test tube, three twisted ratios of the modified and plain twisted tapes, and tapes before twisting. The Solid Work program was used to build the structure of this study. Table 1 shows the dimensions that were used in building the numerical model. Table 2 shows the material properties of the twisted tapes, the entrance, and the test tube used.

Table 1
The dimensions of geometry used in the numerical model

Type element	D (mm)	L (mm)	W (mm)	t (mm)
Test tube	50	1200	----	----
Entrance	50	500	----	----
Twisted tape	----	1200	38	2

Table 2
The material properties of the twisted tapes, the entrance, and the test tube

Materials	Density, $\boldsymbol{\rho}$ [kg/m^3]	Thermal conductivity k [W/(m.K)]	Specific heat *Cp* [J/(kg .K)]
Copper entrance and test tube	8978	387.6	381
Iron twisted tape	8030	16.27	502.48

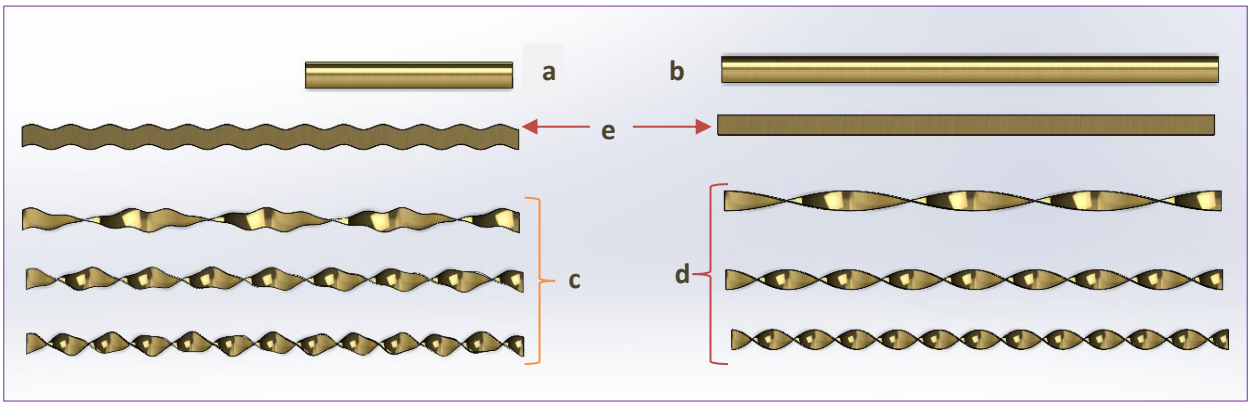

Fig. 1. (a) Entrance, (b) test tube, (c) modified twisted tapes 3TR, (d) plain twisted tape 3TR, and (e) tapes before twisting

3.2 Boundary Conditions

At the tube inlet, uniform velocity profiles were taken into account for water; there were three quantities of velocities Re_{w1}=6300, Re_{w2}=8400, and Re_{w3}= 10500 for air Re_{a1}= 6000, Re_{a2}=10500 and Re_{a3}= 16000. The fluid outlet was at the atmospheric condition, which comprises zero relative gauge pressure and an ambient temperature of 291 K, at the outlet because the pressure outlet boundary condition was applied with an adiabatic test tube wall surrounding, the test tube wall was subjected to a constant heat flux q_1= 2750W/m^2, q_2=4000 W/m^2 and q_3=5250 W/m^2. The internal tube walls are configured to be non-slip, and the outlet condition is static pressure with zero setting.

3.3 Assumptions

The governor equations are solved under the following presumptions [25]:

i. a fully developed, turbulent, incompressible, and steady fluid flow.
ii. Ignore the thermal contact resistance and radiation-induced heat transfer between components.
iii. The characteristics of the fluid and solid domains never change.
iv. Ignore viscous dissipation as well as gravitational force.

3.4 Grid-independent Analysis

In this research, Nusselt's number was considered a variable parameter whose value depended on the number of elements, which was used to validate the accuracy of numerical solutions. The sweep method grid was used for mesh, as shown in Figure 2. The Nu number's stabilizations were considered a standard for calculation convergence. The mesh dependency testing shown in Figure 3 used a turbulence model (R k – ε EWT) with wall heat flux 5250 W/m2 using modified twisted tape. To determine whether the chosen mesh was sufficient, many grid sensitivity tests were performed to ensure that the results were grid-independent, and for this work, 2,350,000 nodes were selected for all the computations.

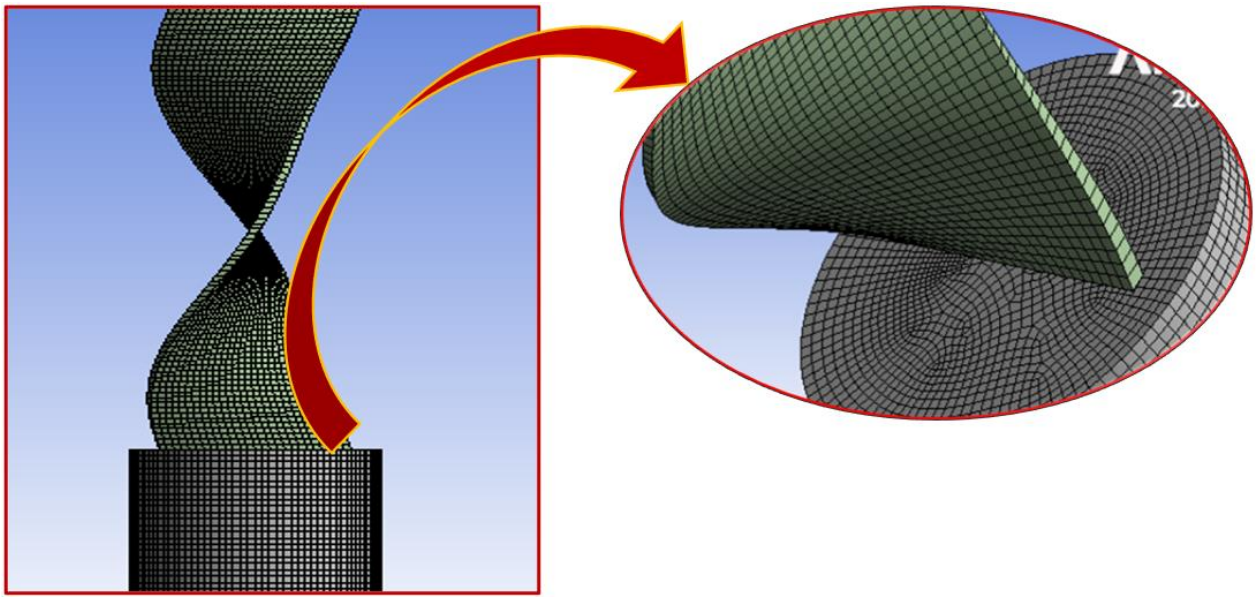

Fig. 2. Mesh with sweep method grid

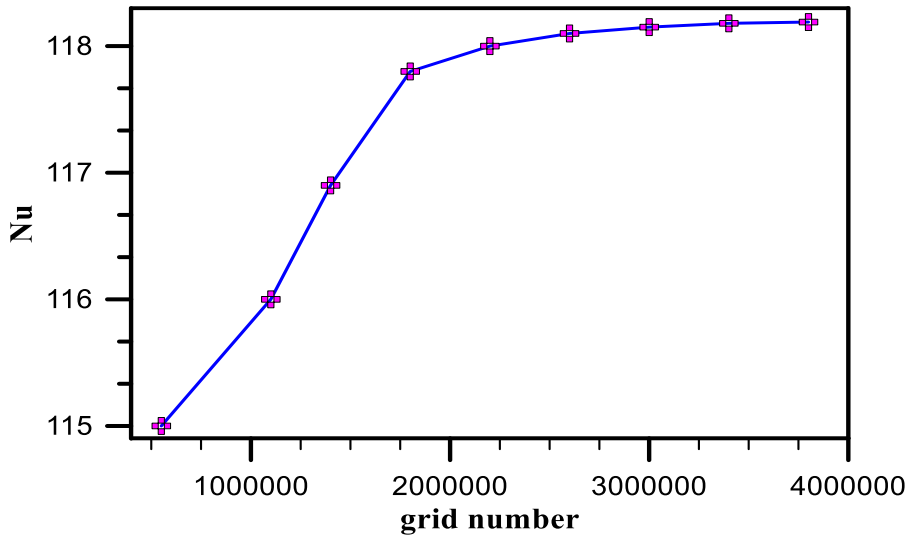

Fig. 3. Mesh independence results by using turbulence model (R k – ε EWT)

3.5 Model Validation

The computational fluid dynamics were validated when compared with numerical results from Mashayekhi *et al.,* [26] for tubes without twisted PT and stationery plain twisted STT, two-phase flow with a Reynolds number range of 250-1000 at a constant wall heat flux of 5000 W/m2. The Root Mean Square error (RMSE) measure was used to assess the agreement between the present work and the results of Mashayekhi *et al.,* [26]. The results for PT were 0.559, and for STT were 0.519. Also, the maximum difference of the Nu number between the results of the present work and the result from Ramin for plain tube was one at Re = 250, while the maximum difference of Nu for tube with stationary twisted tape was 0.7 at Re = 525, corresponding to the Reynolds numbers taken as shown in Figure 4, which is very clear from the comparison between Mashayekhi *et al.,* [26] and the present work that all curves had the same trend for these outcomes, which illustrates the reliability of these models. Figure 5 is a flowchart illustrates the steps followed to build the mathematical and engineering model of the modeling process to solving the CFD simulation model.

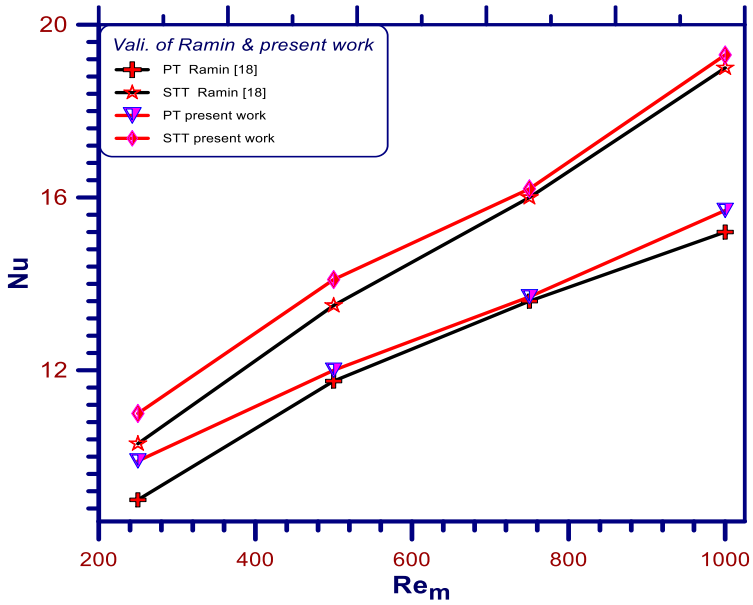

Fig. 4. Validation of Nusselt number between present work and Mashayekhi *et al.,* [26]

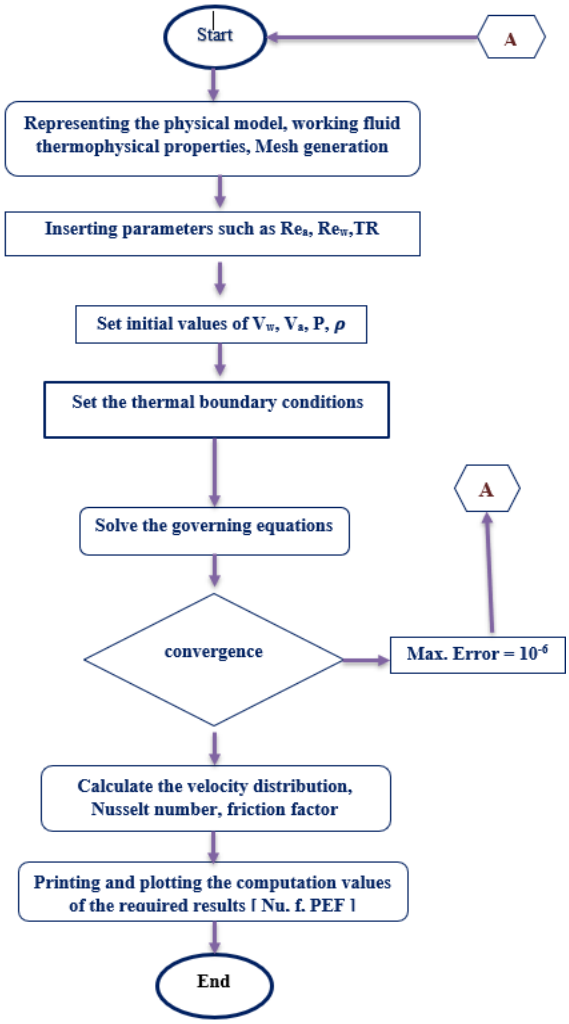

Fig. 5. flowchart of the adopted methodology for solving the CFD simulation model

4. Results and Discussions

4.1 Nusselt Number Variation

Figure 6(a) to Figure 6(c) show a comparison of the Nu numbers values at the range of Re_w (6000 - 10500) when using the plain twisted tape for three twist ratios TR_1, TR_2, TR_3, and at three values of heat flux q_1, q_2, q_3. It is evident that when the twisted tape ratio increases, the enhancement percentage in the average Nusselt number also increases, increasing turbulent flow. This is because the increased swirl flow intensity led to increased centrifugal force, shifting the core flow of mixing fluids toward the heated wall and increasing the contact between the fluid mixture and the hot wall. Also, when the velocity of air and water increases, the Nusselt numbers increase due to the increase in the flowing mass and the turbulent, which increases the heat transfer coefficient according to Eq. (13). We notice from the curves in the figure that the twist ratio has the highest effect on Nusselt, as the highest value obtained in the Figure 6(c), Re_{a3}, TR_3, q_3, and Re_{w3} was 218, while the lowest value in the same conditions was 157 for q_1, TR_1, with an increase rate of 38.8%. As for the modified twisted bar, Figure 7(a) to Figure 7(c) showed a uniform increase of the Nusselt numbers when increasing TR, Re_a, and Re_w heat fluxes and for all cases. The highest value reached (278) in Figure 7(a) at conditions of TR_3, q_3, Re_{a3}, and Re_{w3}, while the lowest value reached (184) under the same conditions and at TR_1, an increase of 52%. In general, the modified twisted tape showed a clear improvement in heat transfer by increasing the Nusselt number compared to the plain twisted tape.

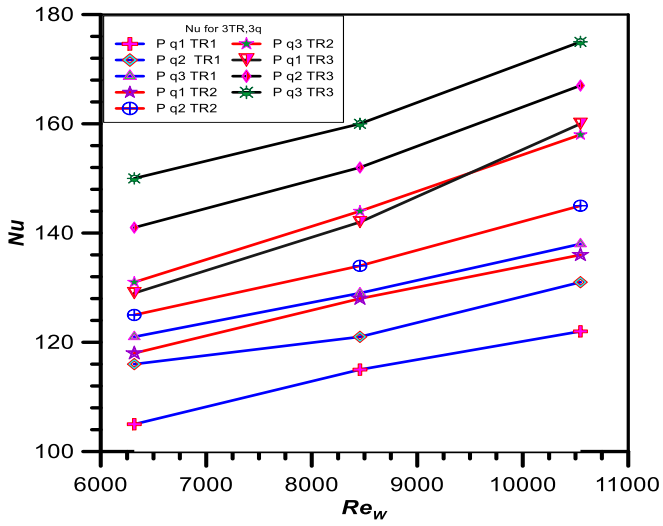

(a) Nu for Qa_1 at dif. Plain TR & dif. Q

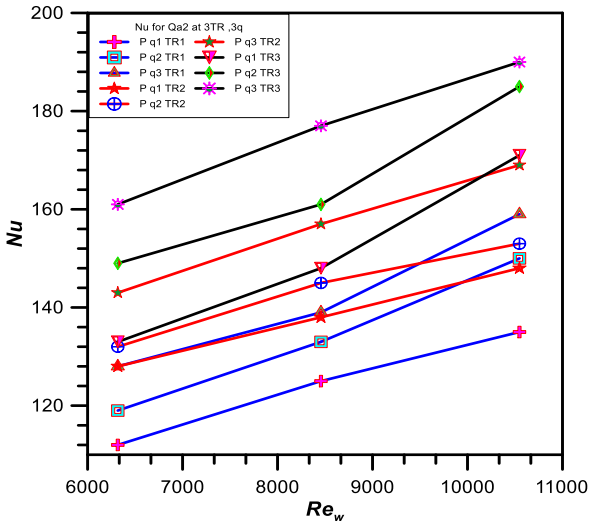

(b) Nu for Q_{a2} at dif. Plain TR & dif. Q

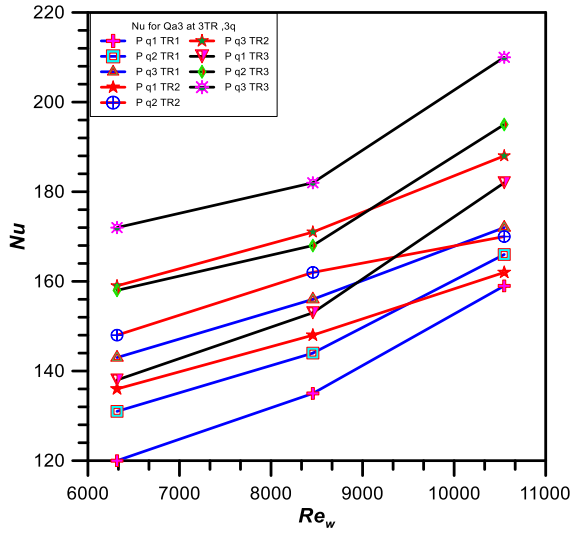

(c) Nu for Q_{a3} at dif. Plain TR & dif. q

Fig. 6. Nu variation in plain twisted

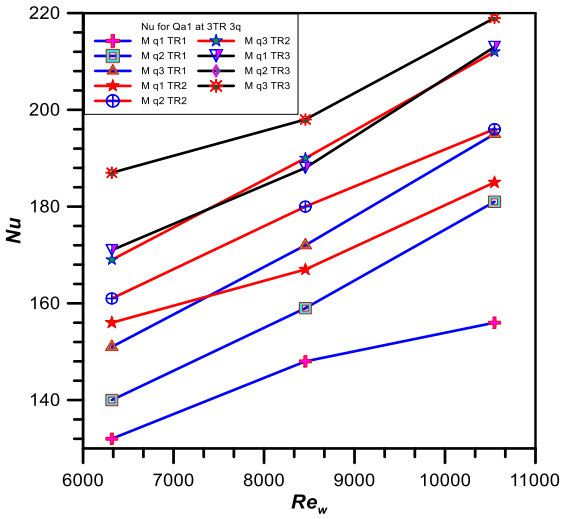

(a) Nu for Qa_1 at dif. Modi. TR & dif. Q

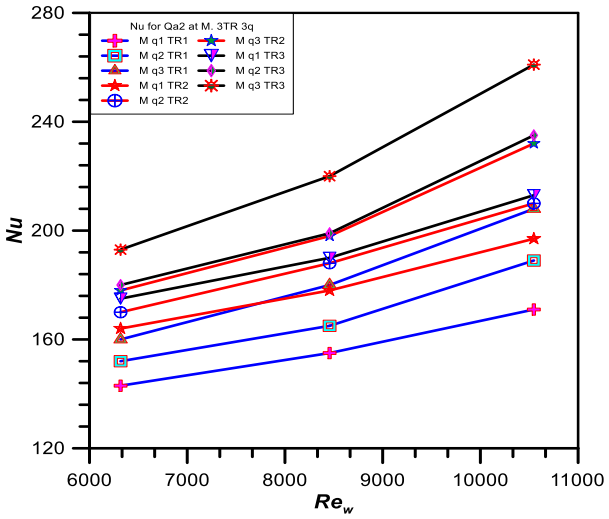

(b) Nu for Q_{a2} at dif. Modi. TR & dif. Q

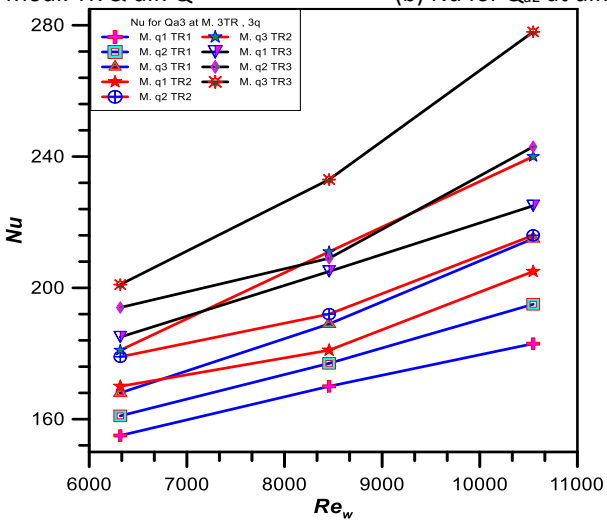

(c) Nu for Q_{a3} at dif. Modi. TR & dif. q

Fig. 7. Nu variation in modified twisted

Figure 8(a) to Figure 8(c) compared the Nusselt numbers between the modified and plain twisted tape at the same twist ratios TR_1 and Re_w = 6000 and the range of Re_a between 6000 and 16000 for three heat flux values. In general, the modified twisted tape showed a clear superiority in the heat transfer process compared with the plain twisted tape for all shapes; this is due to the increase in the amount of heat transferred due to the increase in heat flux through the tube walls. The highest value of the Nusselt number was 218 in Figure 8(c). It was for the modified twisted tape at Re_a = 16000, q_3, while the value of the Nusselt number for the plain twisted tape under the same conditions was 172, with an increase of 26.7%, and it is a good improvement that can be adopted.

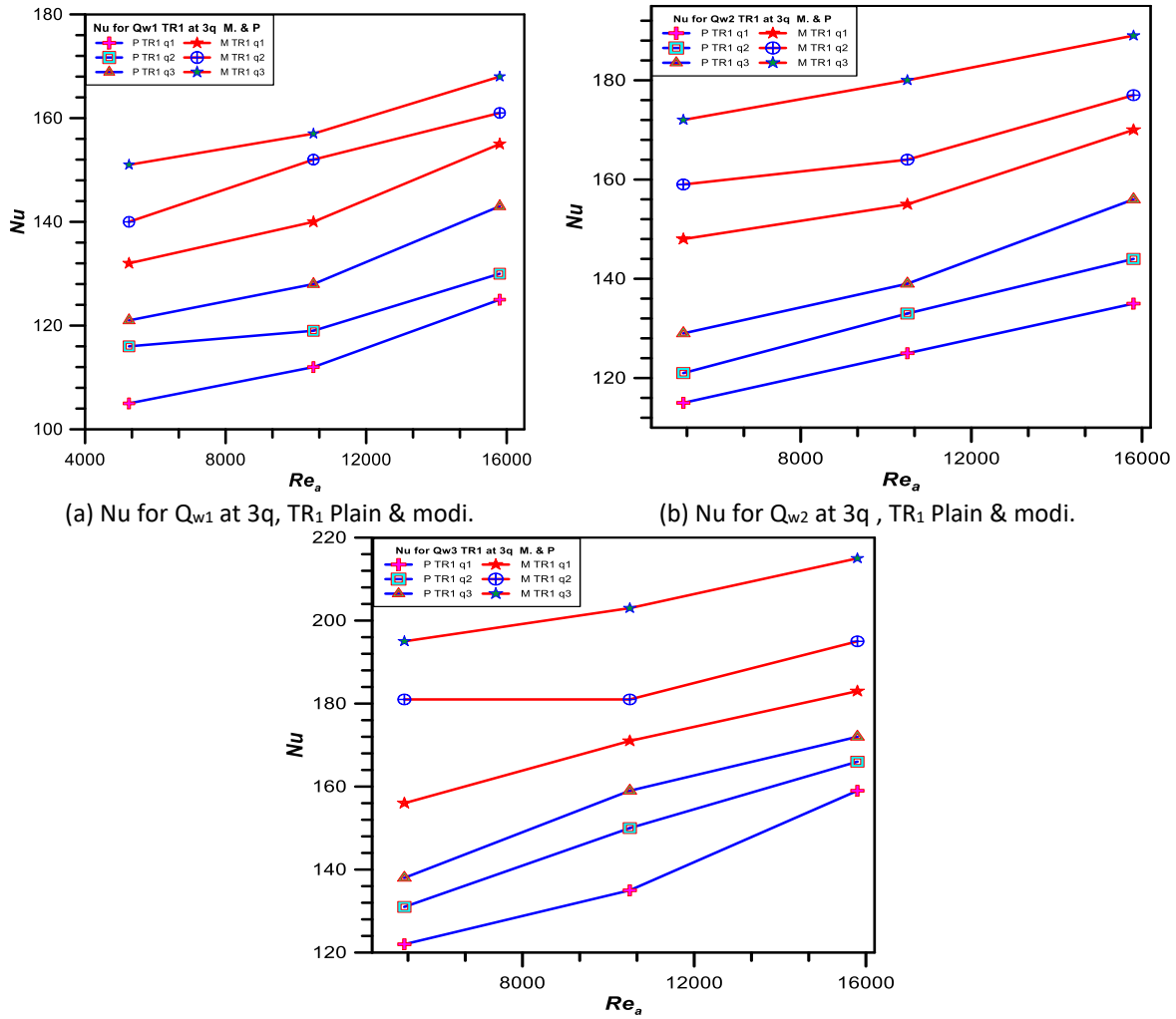

(a) Nu for Q_{w1} at 3q, TR_1 Plain & modi.

(b) Nu for Q_{w2} at 3q , TR_1 Plain & modi.

(c) Nu for Q_{w3} at 3q, TR_1 Plain & modi.

Fig. 8. Comparison of modi. and plain at TR_1

Nusselt numbers for the modified twisted tape and the plain twisted tape with the same twist ratios (TR_1 and Rew = 8450) and the Re_a range (6000–16000) for three different heat flux values were displayed in Figure 9(a) to Figure 9(c). According to Nusselt values, the modified twisted tape demonstrated good heat transfer enhancement for all shapes compared to the plain twisted tape. In Figure 8(c), the modified twisted tape's Nusselt number reached 240 at Re_a = 16000, q_3, while the plain twisted tape's Nusselt number under the same conditions was 186, representing a 29% increase.

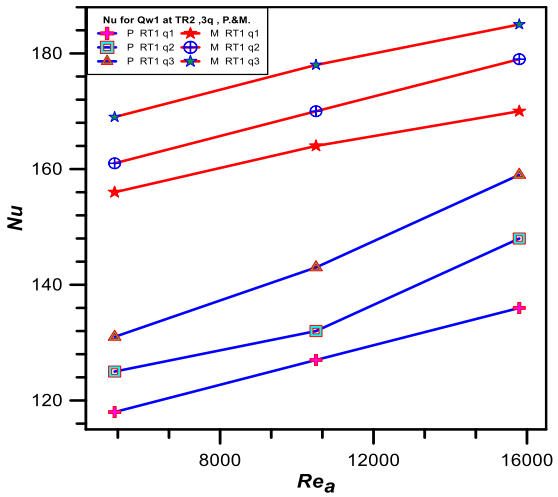

(a) Nu for Q_{w1} at 3q, TR_2 Plain & modi.

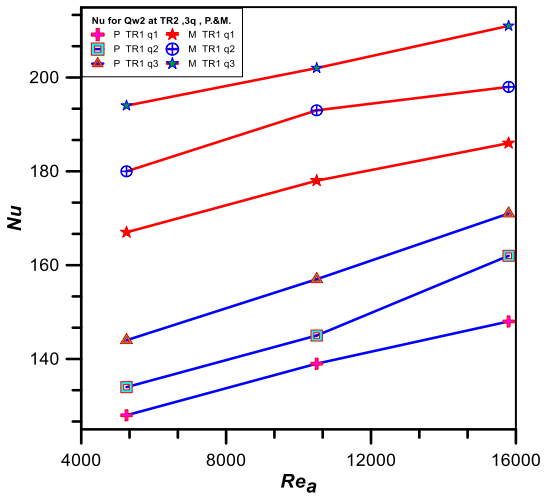

(b) Nu for Q_{w2} at 3q, TR_2 Plain & modi.

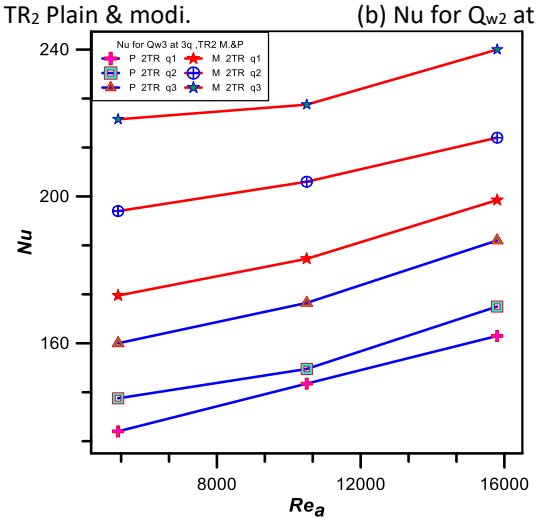

(c) Nu for Q_{w3} at 3q, TR_2 Plain & modi.

Fig. 9. Comparison modi. and plain at TR_2

Figure 10(a) to Figure 10(c) showed a comparison between the modified twisted tape and plain twisted tape for values of Nusselt numbers at the same twist ratios TR_3 and Rew = 10500 for three heat flux values and the range of Re_a between 6000 and 16000. The modified twisted tape showed a high superiority in the heat transfer compared with the plain twisted tape for all cases; this is due to the increase in the amount of heat transferred due to the increase in heat flux through the walls of the tube where the highest value of the Nusselt number 210 in Figure 9(c) was for the plain twisted tape at Re_a = 16000, q_3, while the value of the Nusselt number for the modified twisted tape under the same conditions was 278, with an increase of 28.5%.

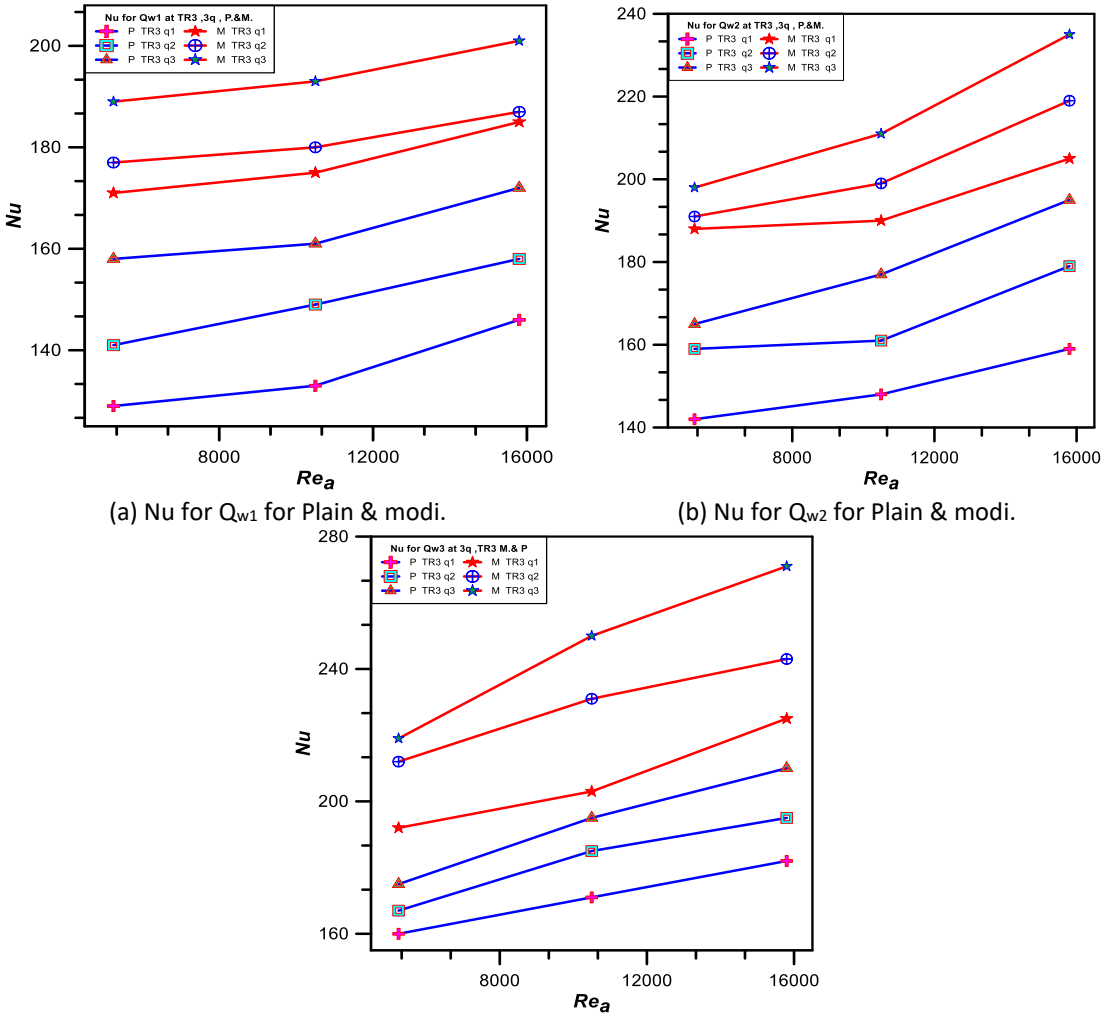

(a) Nu for Q_{w1} for Plain & modi.

(b) Nu for Q_{w2} for Plain & modi.

(c) Nu for Q_{w3} for Plain & modi.

Fig. 10. Comparison between modified twisted and plain at TR_3

4.2 Variation of Friction Factor

Figure 11(a) to Figure 11(c) showed a comparison of the friction factor values at the range of Re_w (6000 - 10500) when using the plain twisted tape for three twist ratios TR_1, TR_2, TR_3, and at three values of heat flux q_1, q_2, q_3. From the results, it is apparent that the average friction factor values increase with increasing twisted tape ratio; the reason for that was that when the twisting rate increases, the collision rate increases between the mixture of flowing fluids (water-air) and the surface of the twisted tape, which acts as a crossbar, leading to an increase in the coefficient of friction. This phenomenon is considered one of the most important defects of twisted tapes. Also, when the velocity of both air and water increases, the friction factor decreases, and the results also indicate a slight decrease in the coefficient of friction when the heat flux increases due to the decrease in the density of the flowing fluids when the temperatures of the test tube walls rise, and this was consistent with Eq. (8). From the curves in Figure 7, the twist ratio has the highest effect on the coefficient of friction compared to the rest of the factors (fluids velocity (water-air), heat flux), as the highest value obtained in Figure 11(a), at Re_{a1}, TR_3, q_1, and Re_{w3} was 0.77, while the lowest value in the same conditions was 0.6 for q_3, TR_1, with a decrease rate of 28.3%.

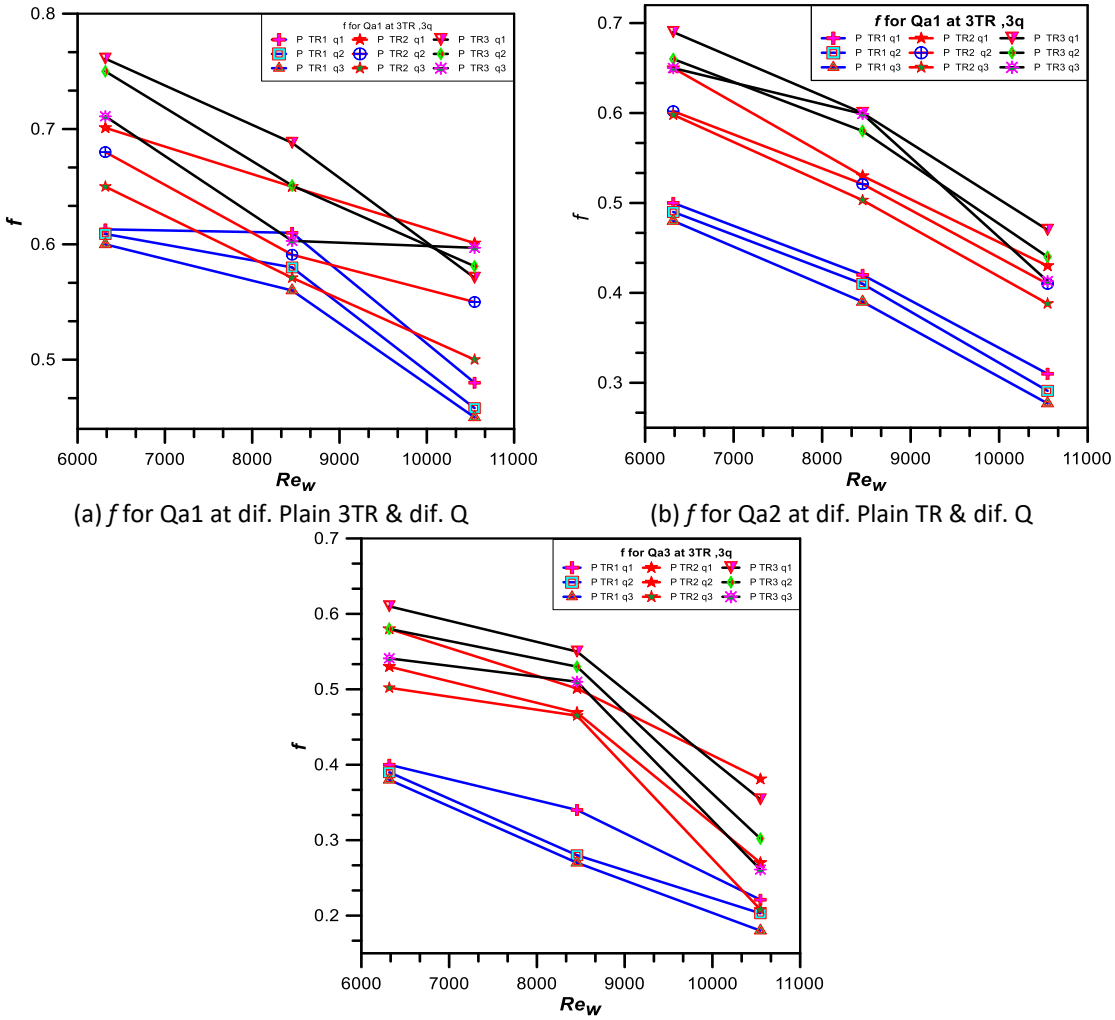

(a) *f* for Qa1 at dif. Plain 3TR & dif. Q

(b) *f* for Qa2 at dif. Plain TR & dif. Q

(c) *f* for Qa3 at dif. Plain TR & dif. Q

Fig. 11. Friction factor variation in plain twisted tape

Figure 12(a) to Figure 12(c) showed a comparison of the friction factor values when using the modified twisted tape for three twist ratios TR_1, TR_2, TR_3, and at three values of heat flux q_1, q_2, q_3 at the range of Rew (6000 - 10500). The results showed that the average friction factor values increase with increasing twisted tape ratio. On the other hand, when the velocity of both air and water increases, the friction factor decreases, and the results also indicate a slight decrease in the friction factor when the heat flux increases. From the curves in Figure 7, the twist ratio has the highest effect on the friction factor compared to the rest of the factors (fluid velocity (water-air), heat flux), and this was the same behaviour as the plain twisted tape, but with lower values for all cases, which was a good indicator add to the modified twisted tape, the highest value obtained in Figure 12(a), at Re_{a1}, TR_3, q_1, and Re_{w3} was 0.62, while the lowest value in the same conditions was 0.51 for q_3, TR_1, with a decrease rate of 21.5 %.

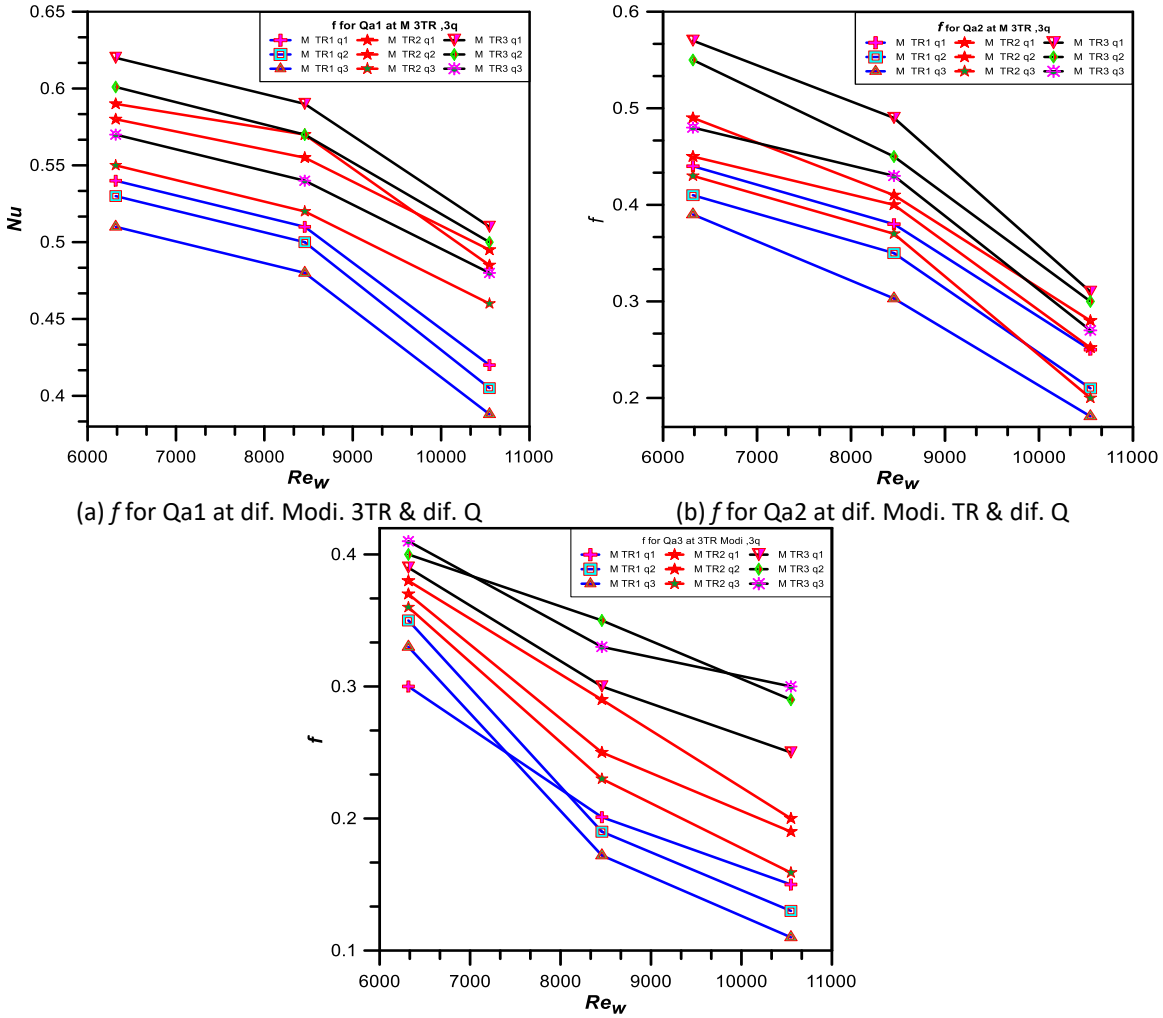

(a) *f* for Qa1 at dif. Modi. 3TR & dif. Q

(b) *f* for Qa2 at dif. Modi. TR & dif. Q

(c) *f* for Qa3 at dif. Modi. TR & dif. Q

Fig. 12. Friction factor variation in modified twisted tape

Figure 13(a) to Figure 13(c) shows a comparison of the friction factor values between the modified and plain twisted tape for a twisted ratio of TR1 and at three values of heat fluxes q1, q2, q3 in the range Rea (6000 - 1600) at Rew1. The results showed that the average value of the friction factor for the modified tape was significantly less than that of the plain twisted tape. The difference in the highest value for the plain twisted tape was 0.62, while the modified twisted tape under the same conditions was 0.55, with a decrease rate of 12.7%.

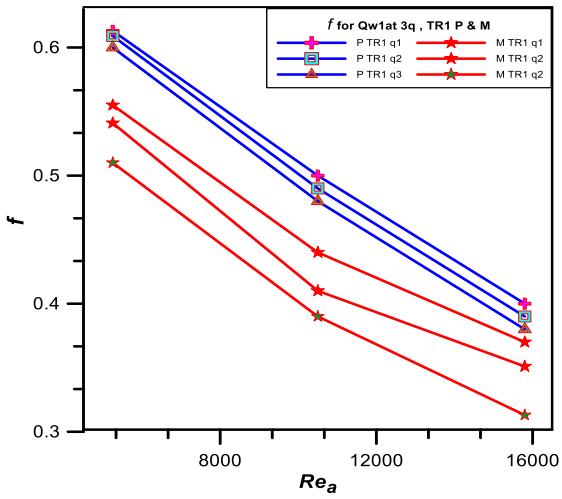

(a) *f* for Qw1 and TR_1 plain and modi.

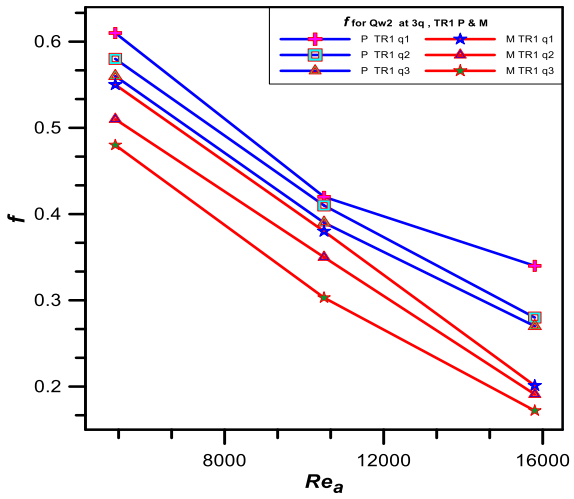

(b) *f* for Qw2 and TR_1 plain and modi.

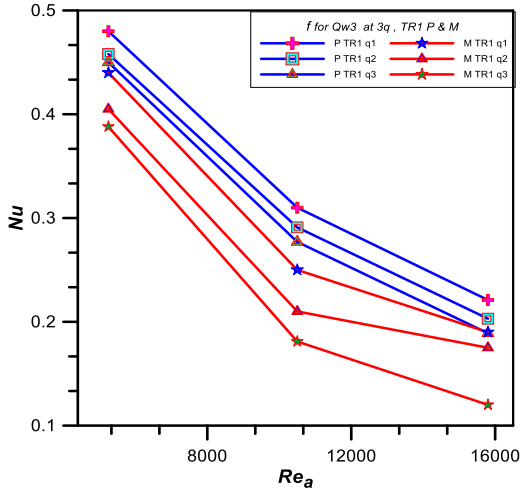

(c) *f* for Qw3 and TR_1 for plain and modi.

Fig. 13. Comparison between modified and plain twisted at TR_1

In Figure 14(a) to Figure 14(c), the friction factor values for the twisted ratio of TR2 and Rew2 under the same conditions as in Figure 8 are compared between the modified and plain twisted tape. According to the results, the modified tape had a lower average friction factor than the plain twisted tape. The modified tape had a decrease rate of 20.7%, whereas the plain twisted tape had the highest value of 0.7 at q1 and Rea1 the modified had 0.58.

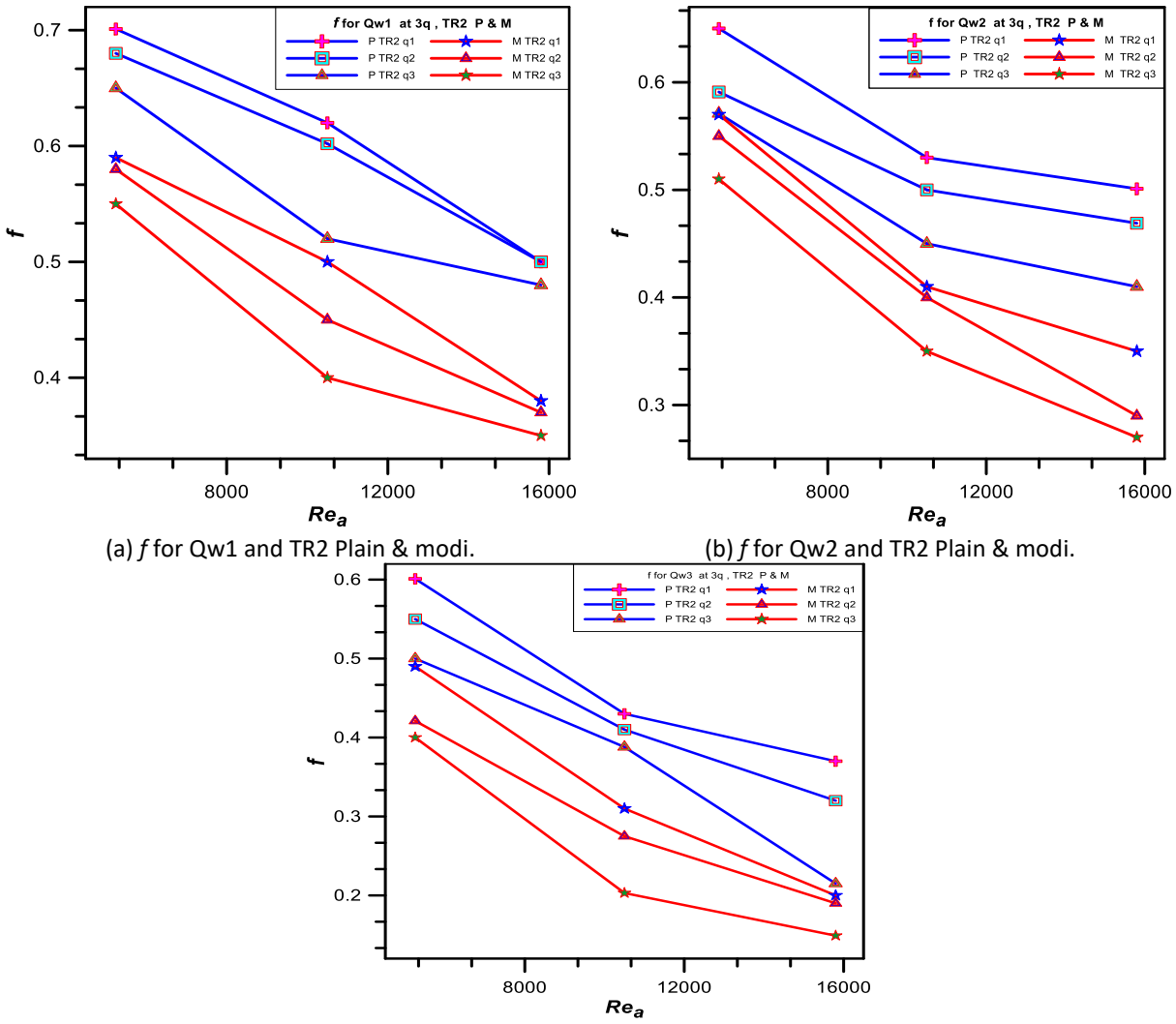

(a) *f* for Qw1 and TR2 Plain & modi.

(b) *f* for Qw2 and TR2 Plain & modi.

(c) *f* for Qw3 and TR2 for Plain & modi.

Fig. 14. Comparison between modified and plain twisted at TR_2

Under the same circumstances in Figure 13, Figure 15(a) to Figure 15(c) compares the friction factor values for the twisted ratio of TR3 at Rew3 between the modified and plain twisted tape. The modified tape had a lower average friction factor than the plain twisted tape, with a 13.1% decrease rate. The plain twisted tape had the highest value of 0.69 at q1 and Rea1, while the modified tape had a 0.61 friction factor at the same conditions.

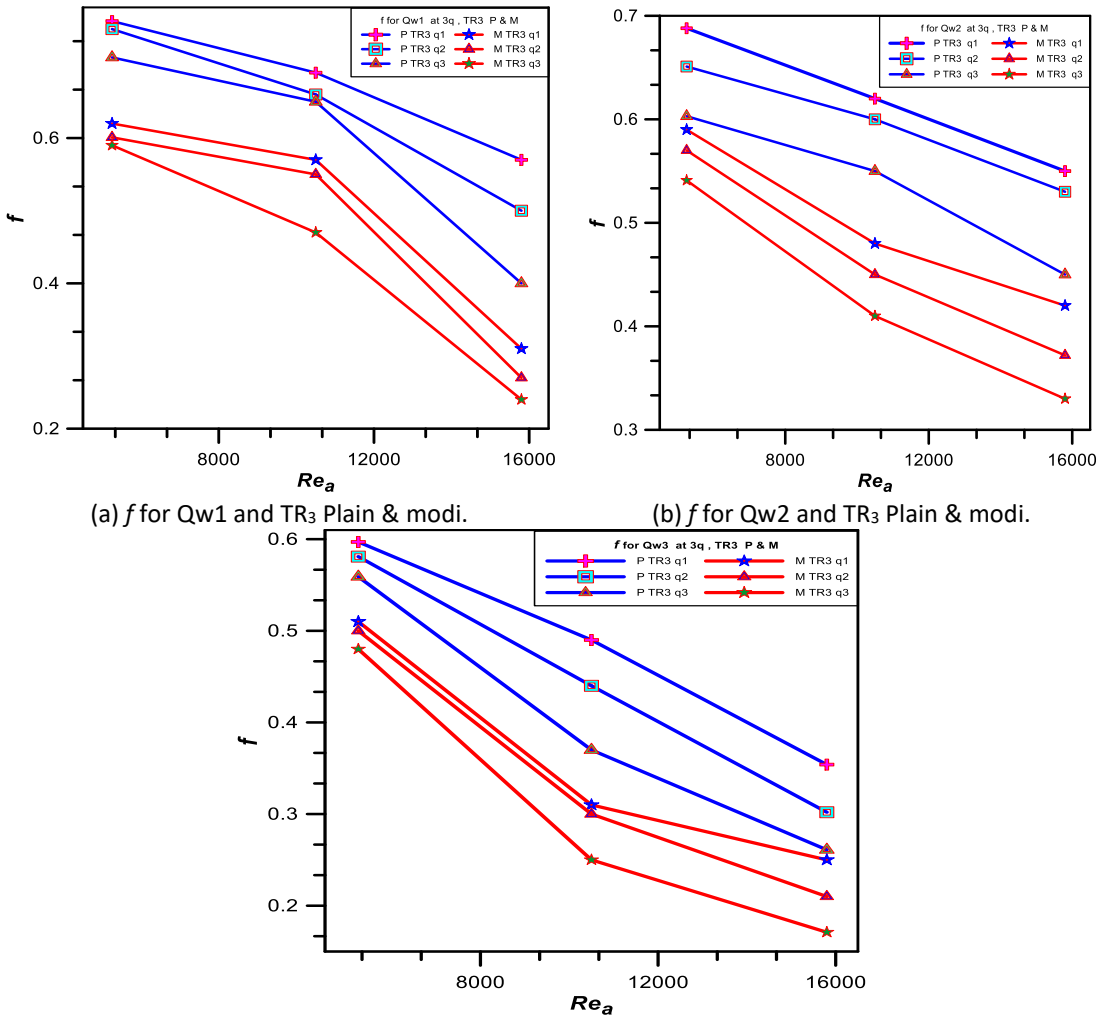

(a) *f* for Qw1 and TR_3 Plain & modi. (b) *f* for Qw2 and TR_3 Plain & modi.

(c) *f* for Qw3 and TR_3 Plain & modi.

Fig. 15. Comparison of friction factor between modified and plain twisted at TR3

4.3 Variation of the Performance Evaluation Factor

The performance evaluation factor is the most important criterion for deciding whether or not heat exchangers can be used. It balances the improvement processes in heat transfer due to using a specific technology (twisted tape inserted in this case), indicated by the Nusselt number. The friction factor indicates the resulting increase in pressure required for flow due to using that technology when the two indicators are divided by the normal condition values without any technology under the same conditions. Figure 16(a) to Figure 16(c) shows the performance evaluation factor values for the plain twisted tape at the range of Rew of 6000 - 10500 for three heat flux values with three twisting ratios and three Rea. The results were close and somewhat overlapping, but in general, it can be said that the highest twisting ratio TR3 achieved the highest performance rating out of the rest of the types, and the reason was the strong effect of the increase in the intensity of the swirling flow generated by the presence of the twisted tape on heat transfer compared to the rest of the factors (heat flux, water, and air velocities). The highest value of the performance evaluation factor was 1.3 at the Rea1, Rew1, and the twist ratio of TR 3, while the lowest value under the same conditions was 0.97, with an increase of 34%.

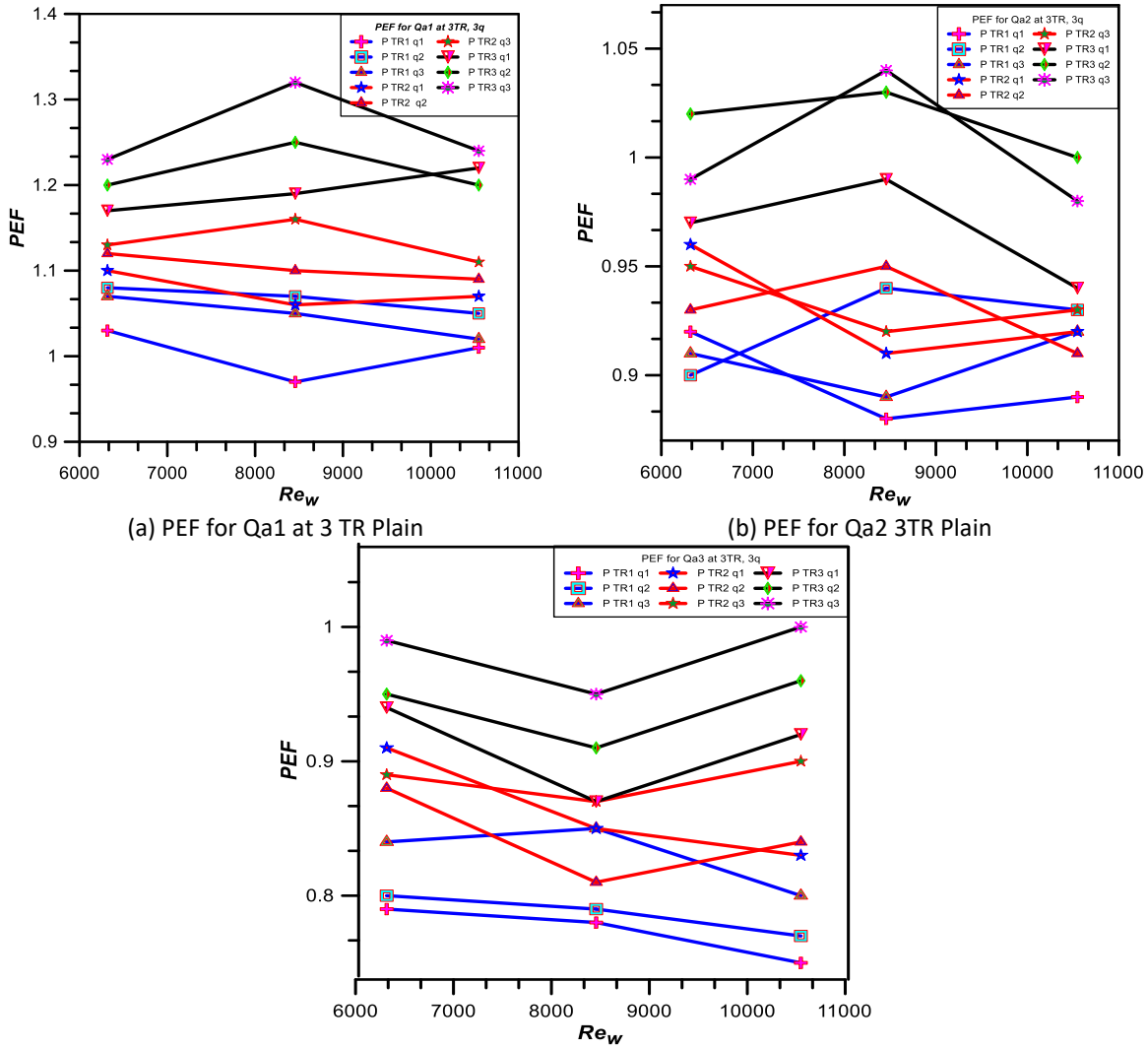

(a) PEF for Qa1 at 3 TR Plain

(b) PEF for Qa2 3TR Plain

(c) PEF for Qa3 3TR Plain

Fig. 16. Performance evaluation factor variation in plain twisted tape

Figure 17(a) to Figure 17(c) show the performance evaluation factor values for the modified twisted tape at the range of Rew 6000 - 10500 for three heat flux values with three twisting ratios and three Rea. The highest value of the performance evaluation factor was 1.88 at the q2, Rea1, Rew1, and the twist ratio of TR 3, while the lowest value under the same conditions was 1.31, with an increase of 43.4 %.

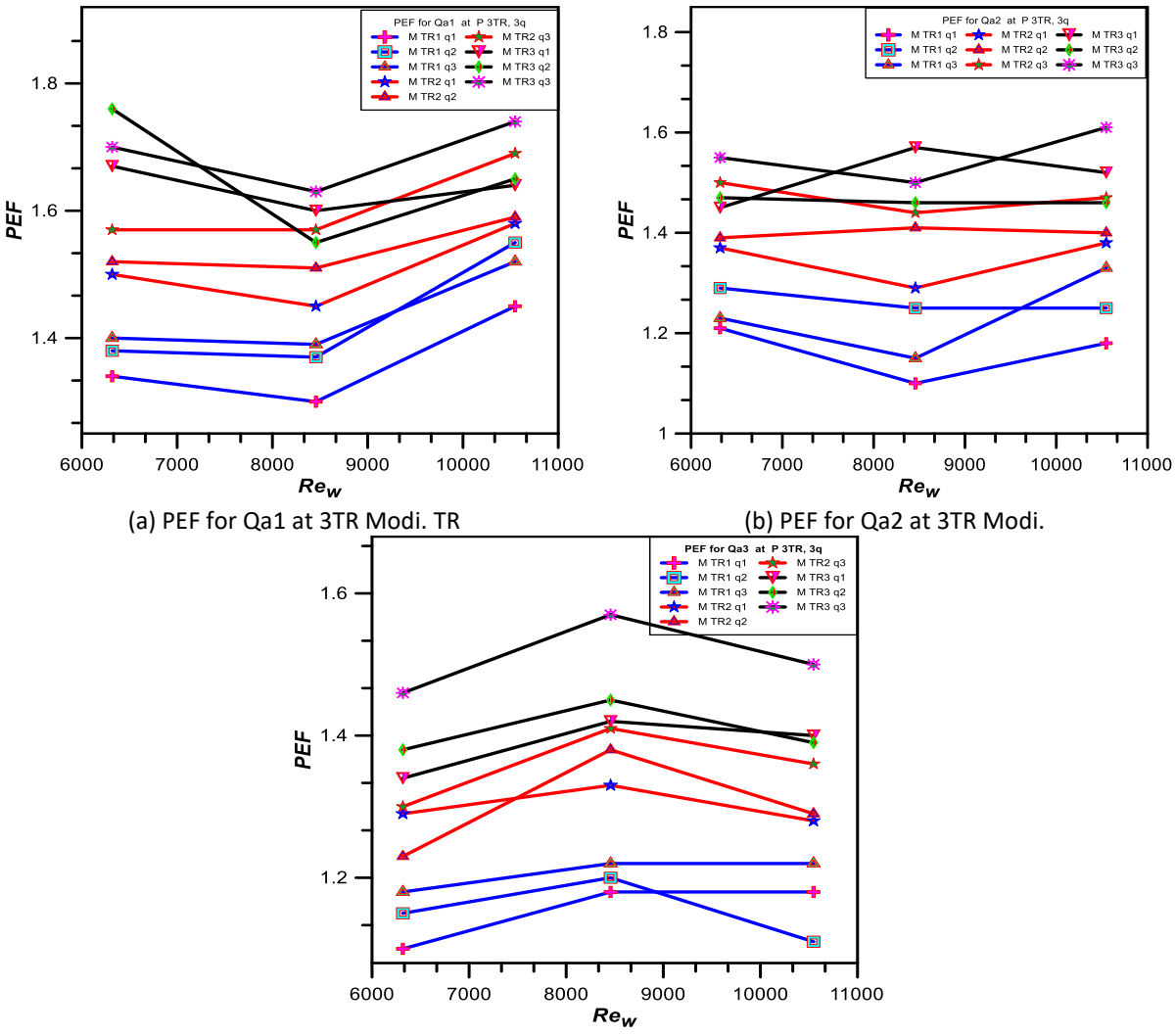

(a) PEF for Qa1 at 3TR Modi. TR

(b) PEF for Qa2 at 3TR Modi.

(c) PEF for Qa3 at 3TR Modi.

Fig. 17. Performance evaluation factor variation in modified twisted tape

Figure 18(a) to Figure 18(c) displays the comparison of the results of the performance evaluation factor values between the modified and ordinary twisted bar at the twist ratio TR 1 with three values of Rea for each case with three values of heat flux and a Rew range of 6000-16000. The results showed that the modified twisted tape was superior to the plain twisted tape by a large and noticeable difference for all values and all cases, as the highest value obtained for the modified twisted tape was 1.51 in case C at Q3, Rew1, while the highest value obtained for the plain twisted tape was 1.2 in same conditions, an increase of 25.8%, which was a strong and positive indicator of the efficiency of the modified twisted tape.

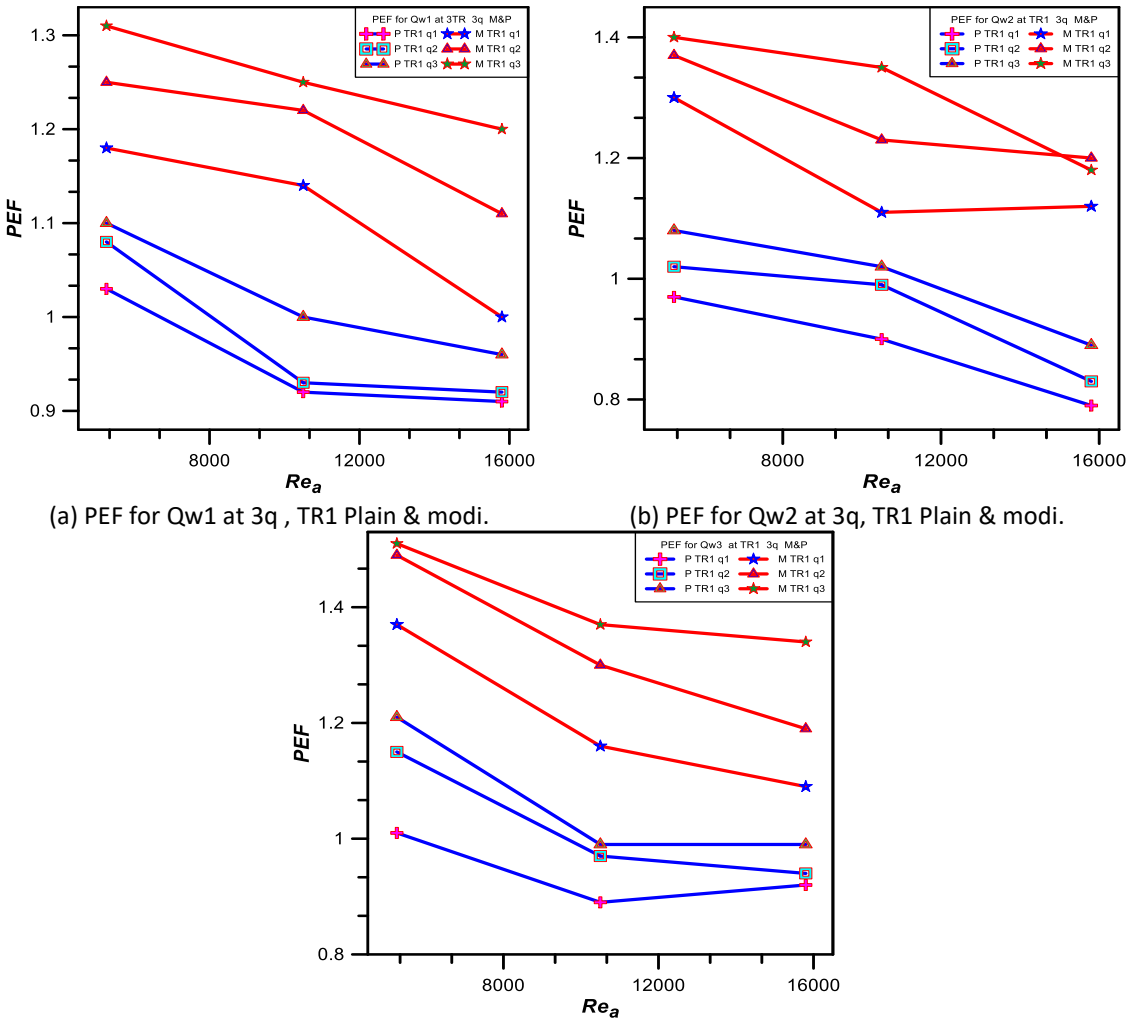

(a) PEF for Qw1 at 3q , TR1 Plain & modi.

(b) PEF for Qw2 at 3q, TR1 Plain & modi.

(c) PEF for Qw3 at 3q, TR1 Plain & modi.

Fig. 18. Comparison between modified and plain twisted at TR1

The comparison of the modified and plain twisted tapes performance evaluation factor values at the twist ratio TR_2 with three values of Re_w for each case with three values of heat flux and a Rea range of 6000-16000 was shown in Figure 19(a) to Figure 19(c). The highest value obtained for the modified twisted tape was 2 in case b at Q_3, Re_{w2}, while the highest value obtained for the ordinary twisted tape was 1.01, with an increase of 81.8% under the same conditions. The results demonstrated that the modified twisted tape outperformed the plain twisted tape by a significant and noticeable difference for all values and cases, which was a very significant and encouraging sign to adopt the modified twisted tape.

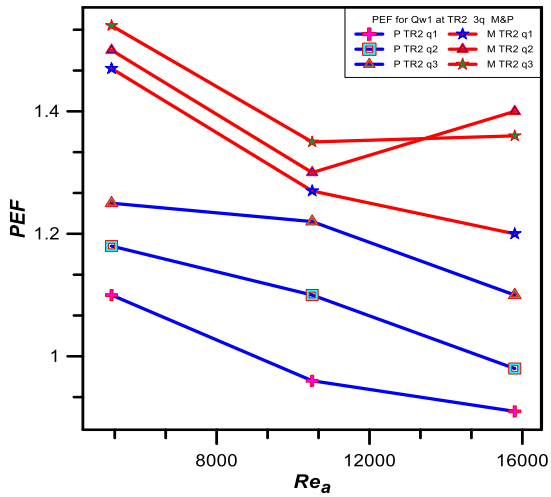

(a) PEF for Qw1 at 3q, TR2 Plain & modi.

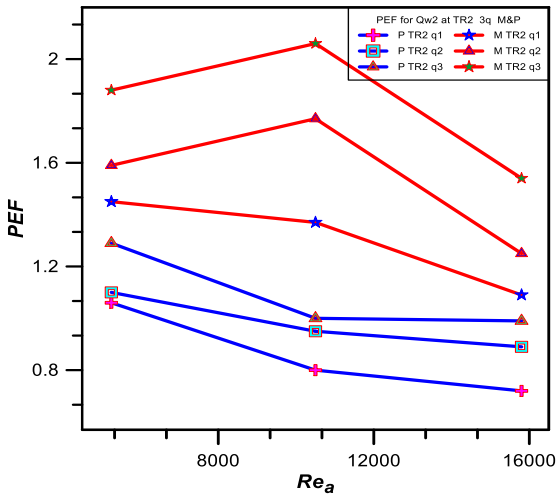

(b) PEF for Qw2 at 3q, TR2 Plain & modi.

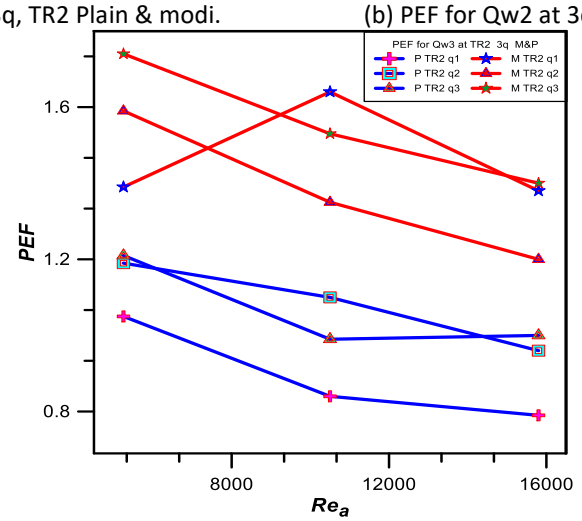

(c) PEF for Qw3 at 3q, TR2 Plain & modi.

Fig. 19. Comparison between modified and plain twisted at TR2

Figure 20(a) to Figure 20(c) compares the performance evaluation factor values results between the modified and plain twisted tape at the twist ratio TR_3 under the same conditions as Figure 14. The modified twisted tape outperformed the plain twisted tape by a noticeable difference for all values and all cases, as the highest value obtained for the modified twisted tape was 1.78 in case an at Q2 Rew1, while the highest value obtained for the plain twisted tape was 1.21 under the same conditions with an increase of 48.3 %.

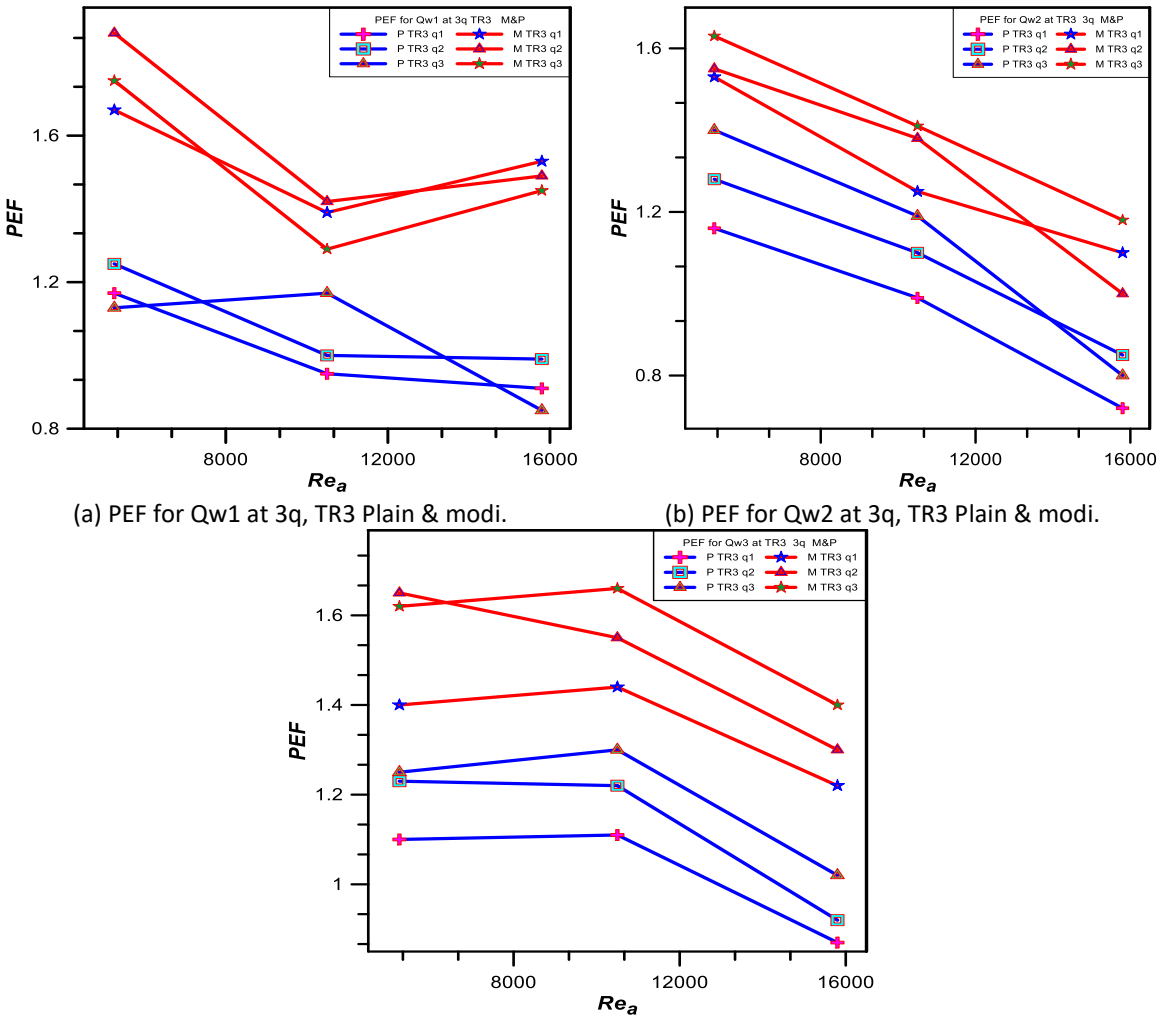

(a) PEF for Qw1 at 3q, TR3 Plain & modi.

(b) PEF for Qw2 at 3q, TR3 Plain & modi.

(c) PEF for Qw3 at 3q, TR3 Plain & modi.

Fig. 20. Comparison between modified and plain twisted at TR3

The results presented in Figure 14, Figure 15, and Figure 16 clearly and strongly demonstrated that the work of the modified twisted tape in improving heat transfer for two-phase flow in vertical pipes was good and can be adopted in applications despite the presence of pressure losses as a result of the use of the tape. However, improving heat transfer efficiency kept the performance evaluation factor high.

5. Conclusions

This study aimed to enhance heat transfer and minimize the pressure drop in two-phase flow across tubes by altering the geometry of the twisted tapes inserted and choosing the optimal design of twisted tape with a wavy edge that increases turbulence intensity and higher mixing of liquid. The present work has been done with three different geometrical cases, namely: (I) a pipe without a twisted tape, (ii) a pipe with a plain twisted tape, and (iii) a pipe with a modified twisted tape with a wavy edge. The effects of water and air flow velocities, twisted ratio, and heat flux on the Nusselt number, friction factor, and performance evaluation factor have been analyzed for all cases. The results confirmed that:

i. When the amounts of heat fluxes and the Reynolds numbers of water or air increased, the Nusselt number and the friction factor decreased in all cases.

ii. When using twisted tapes (plain or modified), the Nusselt number improved significantly, but at the same time, the coefficient of friction also increased. It was observed that the introduction of the twisted tape led to increased turbulence intensity, increased vortex generation, and converted the flow into vortex flow.
iii. The modified twisted tape has proven to be highly effective in improving heat transfer compared to the plain twisted tape under all conditions and for all cases, as the highest value of Nusselt number reached 278 for the modified, while for the plain was only 210, with an increase of 28.5% at TR3, Rew3, Rea3, q3.
iv. The friction factor increased when the twisted tape of all types was inserted. It also increased as the twisted ratio decreased, but, in general, the modified twisted tape was found to reduce the friction factor compared to plain tape, as the highest value for the plain was 0.62, while for the modified under the same conditions was 0.55, with a decrease rate of 12.7%.
v. The highest value obtained for PEF for the modified twisted tape was 2, while for the plain twisted tape was 1.01, with an increase of 81.8% under the same conditions.
vi. In general, there was more thermal enhancement when reducing the tape twisted ratio, as the highest value of Nu for the plain twisted for TR3 was 210 at Rew3, Rea3, q3, while the lowest at TR1 was 175 at the same conditions. For the modified twisted under the same conditions, the highest at TR3 was 278, while the lowest at TR1 was 220.

Understanding the effect of the mentioned modifications was important to heat enhancement in applying two-phase flow in many thermal industrial processes, such as heat exchangers.

6. Scope for Future Work

According to a critical review and results, there has not been much research done on the following twisted bar shapes, though future studies on them should be more interesting:

i. Variable cross-section twisted tapes as opposed to plane ones.
ii. Several coaxial cross-twisted tapes featuring various perforated inserts (oval, rhombic, and square).
iii. Standard twisted tapes with edges that are regularly zigzag.

Acknowledgement

This research was not funded by any grant.

References

[1] Al-Kbodi, Basher Hassan, Taha Rajeh, Mohamed E. Zayed, Yang Li, Jun Zhao, Jiahui Wu, and Yuanyuan Liu. "Transient heat transfer simulation, sensitivity analysis, and design optimization of shallow ground heat exchangers with hollow-finned structures for enhanced performance of ground-coupled heat pumps." *Energy and Buildings* 305 (2024): 113870. https://doi.org/10.1016/j.enbuild.2023.113870

[2] Jia, Li-Chuan, Yi-Fei Jin, Jun-Wen Ren, Li-Hua Zhao, Ding-Xiang Yan, and Zhong-Ming Li. "Highly thermally conductive liquid metal-based composites with superior thermostability for thermal management." *Journal of Materials Chemistry C* 9, no. 8 (2021): 2904-2911. https://doi.org/10.1039/D0TC05493C

[3] Attia, Mohammed El Hadi, Mohamed E. Zayed, A. E. Kabeel, Abdelkrim Khelifa, Müslüm Arıcı, and Mohamed Abdelgaied. "Design and performance optimization of a novel zigzag channeled solar photovoltaic thermal system: Numerical investigation and parametric analysis." *Journal of Cleaner Production* 434 (2024): 140220. https://doi.org/10.1016/j.jclepro.2023.140220

[4] Zhu, Danlei, Bo Wang, Hengrui Ma, and Hongxia Wang. "Evaluating the vulnerability of integrated electricity-heat-gas systems based on the high-dimensional random matrix theory." *CSEE Journal of Power and Energy Systems* 6, no. 4 (2019): 878-889.

[5] Wang, Qing, Bowen Liu, and Zhichao Wang. "Investigation of heat transfer mechanisms among particles in horizontal rotary retorts." *Powder Technology* 367 (2020): 82-96. https://doi.org/10.1016/j.powtec.2020.03.042
[6] Rajeh, Taha, Basher Hassan Al-Kbodi, Mohamed E. Zayed, Yang Li, Jun Zhao, and Shafiqur Rehman. "Local entropy generation optimization and thermodynamic irreversibility analysis of oval-shaped coaxial ground heat exchangers: A detailed numerical investigation." *International Journal of Heat and Mass Transfer* 228 (2024): 125650. https://doi.org/10.1016/j.ijheatmasstransfer.2024.125650
[7] Deepika, Kumari, and R. M. Sarviya. "Application based review on enhancement of heat transfer in heat exchangers tubes using inserts." *Materials Today: Proceedings* 44 (2021): 2362-2365. https://doi.org/10.1016/j.matpr.2020.12.436
[8] Umar, F. O., J. T. Oh, and A. S. Pamitran. "Two-Phase Flow Boiling Pressure Drop with R290 in Horizontal 3 mm Diameter Mini Channel." *Journal of Advanced Research in Experimental Fluid Mechanics and Heat Transfer* 4, no. 1 (2021): 1-7.
[9] Rohaizan, Muhammad Hazeer Khiralsaleh Mohamad, Nor Azwadi Che Sidik, and Kamyar Shameli. "Numerical Analysis of Heat Transfer in Microchannel Heat Transfer in Microchannel Heat Sink using Flow Disruption." *Journal of Advanced Research Design* 106, no. 1 (2023): 1-13. https://doi.org/10.37934/ard.106.1.113
[10] Bhagwat, Swanand M., and Afshin J. Ghajar. "Experimental investigation of non-boiling gas-liquid two phase flow in downward inclined pipes." *Experimental Thermal and Fluid Science* 89 (2017): 219-237. https://doi.org/10.1016/j.expthermflusci.2017.08.020
[11] Khorasani, Saleh, and Abdolrahman Dadvand. "Effect of air bubble injection on the performance of a horizontal helical shell and coiled tube heat exchanger: An experimental study." *Applied Thermal Engineering* 111 (2017): 676-683. https://doi.org/10.1016/j.applthermaleng.2016.09.101
[12] Demong, Ariny, Andrew Ragai Rigit, and Khairuddin Sanaullah. "Effect of Swirl Gas Injection on Bubble Characteristics in a Bubble Column." *Journal of Advanced Research in Fluid Mechanics and Thermal Sciences* 102, no. 2 (2023): 155-165. https://doi.org/10.37934/arfmts.102.2.155165
[13] Liu, Wen, Xiaofei Lv, Sheng Jiang, Huazheng Li, Hao Zhou, and Xiangji Dou. "Two-phase flow pattern identification in horizontal gas-liquid swirling pipe flow by machine learning method." *Annals of Nuclear Energy* 183 (2023): 109644. https://doi.org/10.1016/j.anucene.2022.109644
[14] Singh, Dwesh K., Waquar Ahmad, and Rajan Kumar. "Two phase nanofluid flow and heat transfer characteristics in smooth horizontal tube installed by twisted tapes with alternate axes of rotation." *Journal of the Brazilian Society of Mechanical Sciences and Engineering* 43 (2021): 1-17. https://doi.org/10.1007/s40430-021-03253-5
[15] Alnasur, Fawzi Sh, Ahmed Ch Almansoori, Mushtaq A. AL-Furaiji, and Muhammed Im Kareem. "A Study of the Chemical and Physical Properties of Cane as a Biofuel After Thermal Treatment Processes (Tarification)." In *Journal of Physics: Conference Series*, vol. 1664, no. 1, p. 012133. IOP Publishing, 2020. https://doi.org/10.1088/1742-6596/1664/1/012133
[16] Mustafa, Jawed, Saeed Alqaed, Hikmet Ş. Aybar, and Shahid Husain. "Investigation of the effect of twisted tape turbulators on thermal-hydraulic behavior of parabolic solar collector with polymer hybrid nanofluid and exergy analysis using numerical method and ANN." *Engineering Analysis with Boundary Elements* 144 (2022): 81-93. https://doi.org/10.1016/j.enganabound.2022.08.011
[17] Zhao, Jinguo, Shaker A. Reda, Khaled S. Al-Zahrani, Pradeep Kumar Singh, Majdi Talal Amin, Elyased Tag-Eldin, and Faezeh Emami. "Hydro-thermal and economic analyses of the air/water two-phase flow in a double tube heat exchanger equipped with wavy strip turbulator." *Case Studies in Thermal Engineering* 37 (2022): 102260. https://doi.org/10.1016/j.csite.2022.102260
[18] Jadhav, Swati, Manojkumar Hambarde, Ramakant Shrivastava, and Gopal Nandan. "Pressure drop prediction in flow boiling of R-407C in two phase flow using twisted tape insert in horizontal tube." In *AIP Conference Proceedings*, vol. 2341, no. 1. AIP Publishing, 2021. https://doi.org/10.1063/5.0050373
[19] Tarasevich, S. E., A. B. Yakovlev, A. A. Giniyatullin, and A. V. Shishkin. "Heat and mass transfer in tubes with various twisted tape inserts." In *ASME International Mechanical Engineering Congress and Exposition*, vol. 54969, pp. 697-702. 2011. https://doi.org/10.1115/IMECE2011-62088
[20] Pourahmad, Saman, S. M. Pesteei, Hamze Ravaeei, and Saleh Khorasani. "Experimental study of heat transfer and pressure drop analysis of the air/water two-phase flow in a double tube heat exchanger equipped with dual twisted tape turbulator: Simultaneous usage of active and passive methods." *Journal of Energy Storage* 44 (2021): 103408. https://doi.org/10.1016/j.est.2021.103408
[21] Moghaddam, Hadi Ahmadi, Alireza Sarmadian, Amirmasoud Asnaashari, Hossein Ahmadi Nejad Joushani, Mohammad Saidul Islam, Suvash C. Saha, Golara Ghasemi, and Maziar Shafaee. "Condensation heat transfer and pressure drop characteristics of Isobutane in horizontal channels with twisted tape inserts." *International Journal of Refrigeration* 118 (2020): 31-40. https://doi.org/10.1016/j.ijrefrig.2020.06.019

[22] Sajadi, B., M. Soleimani, M. A. Akhavan-Behabadi, and E. Hadadi. "The effect of twisted tape inserts on heat transfer and pressure drop of R1234yf condensation flow: An experimental study." *International Journal of Heat and Mass Transfer* 146 (2020): 118890. https://doi.org/10.1016/j.ijheatmasstransfer.2019.118890

[23] Sarmadian, Alireza, Hadi Ahmadi Moghaddam, Amirmasoud Asnaashari, Hossein Ahmadi Nejad Joushani, Mostafa Moosavi, Mohammad S. Islam, Suvash C. Saha, and Maziar Shafaee. "Flow boiling heat transfer and pressure drop characteristics of Isobutane in horizontal channels with twisted tapes." *International Journal of Heat and Mass Transfer* 162 (2020): 120345. https://doi.org/10.1016/j.ijheatmasstransfer.2020.120345

[24] Yan, Jianguo, Qincheng Bi, Ge Zhu, Laizhong Cai, Qizheng Yuan, and Haicai Lv. "Critical heat flux of highly subcooled water flow boiling in circular tubes with and without internal twisted tapes under high mass fluxes." *International Journal of Heat and Mass Transfer* 95 (2016): 606-619. https://doi.org/10.1016/j.ijheatmasstransfer.2015.12.024

[25] Rao, Yongchao, Zehui Liu, Shuli Wang, and Lijun Li. "Numerical Simulation on the Flow Pattern of a Gas-Liquid Two-Phase Swirl Flow." *ACS Omega* 7, no. 3 (2022): 2679-2689. https://doi.org/10.1021/acsomega.1c05144

[26] Mashayekhi, Ramin, Hossein Arasteh, Pouyan Talebizadehsardari, Apurv Kumar, Morteza Hangi, and Alireza Rahbari. "Heat transfer enhancement of nanofluid flow in a tube equipped with rotating twisted tape inserts: A two-phase approach." *Heat Transfer Engineering* 43, no. 7 (2022): 608-622. https://doi.org/10.1080/01457632.2021.1896835

[27] Wang, Jiaxin, Wenxing Ma, Chunbao Liu, Hongchao Fu, Liyong Ma, and Jianlin Chen. "Numerical simulation and experimental study of gas-liquid two-phase flow pattern of hydrodynamic retarder." *AIP Advances* 12, no. 10 (2022). https://doi.org/10.1063/5.0095740

[28] Al-Furaiji, Mushtaq A., Fawzi Sh Alnasur, and Muhammed Im Kareem. "Regeneration equations for the Rankine cycle with super-heated steam." In *IOP Conference Series: Earth and Environmental Science*, vol. 1029, no. 1, p. 012015. IOP Publishing, 2022. https://doi.org/10.1088/1755-1315/1029/1/012015

[29] Kanizawa, Fabio Toshio, Taye Stephen Mogaji, and Gherhardt Ribatski. "Evaluation of the heat transfer enhancement and pressure drop penalty during flow boiling inside tubes containing twisted tape insert." *Applied Thermal Engineering* 70, no. 1 (2014): 328-340. https://doi.org/10.1016/j.applthermaleng.2014.05.029

[30] Abid Allah H., Nehad, Fawzi Sh. Alnasur, Ammar Abdulkadhim, Isam Mejbel Abed, Nejla Mahjoub Said, and Azher M. Abed. "MHD natural convection in a wavy nanofluid enclosure with an internally corrugated porous cylinder." *Journal of Taibah University for Science* 18, no. 1 (2024): 2335685. https://doi.org/10.1080/16583655.2024.2335685

[31] Ibrahim, Adnan Q., and Riyadh S. Alturaihi. "Experimental work for single-phase and two-phase flow in duct banks with vortex generators." *Results in Engineering* 15 (2022): 100497. https://doi.org/10.1016/j.rineng.2022.100497

[32] Chen, Desheng, and Zhe Lin. "Numerical Investigation of Gas-Liquid Two-Phase Flow in a Swirl Meter." *MAPAN* 36, no. 3 (2021): 521-532. https://doi.org/10.1007/s12647-021-00468-8

[33] Azizi, Zahra, Vahid Rostampour, Samad Jafarmadar, Saleh Khorasani, and Behzad Abdzadeh. "Performance evaluation of horizontal straight tube equipped with twisted tape turbulator, with air-water two-phase flow as working fluid." *Journal of Thermal Analysis and Calorimetry* 147, no. 6 (2022): 4339-4353. https://doi.org/10.1007/s10973-021-10809-z